Supplementary Information (SI) for

New strategies for submicron characterization the carbon binding of reactive minerals in long-term contrasting fertilized soils: Implications for soil carbon storage

Jian Xiao et al.

* *Correspondence to*: G. H. Yu (yuguanghui@njau.edu.cn or gyu6@ncsu.edu)

Fig. S1 Field fertilization layout and extracted soil (Ferralic Cambisol) colloids from three 24-year (1990-2014) long-term fertilization treatments. Control, no fertilization; NPK, chemical nitrogen, phosphorus and potassium fertilization; NPKM, chemical NPK plus swine manure fertilization.

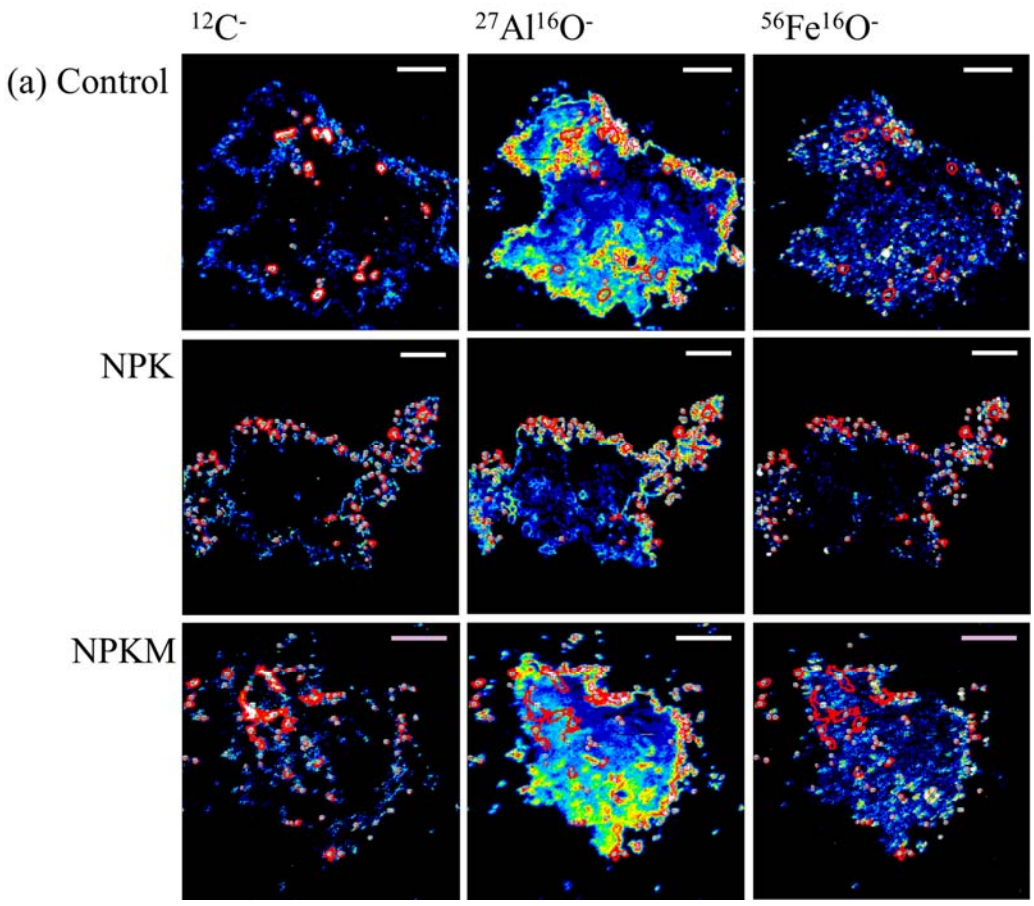
$^{12}C^-$
$^{27}Al^{16}O^-$
$^{56}Fe^{16}O^-$
(a) Control
NPK
NPKM

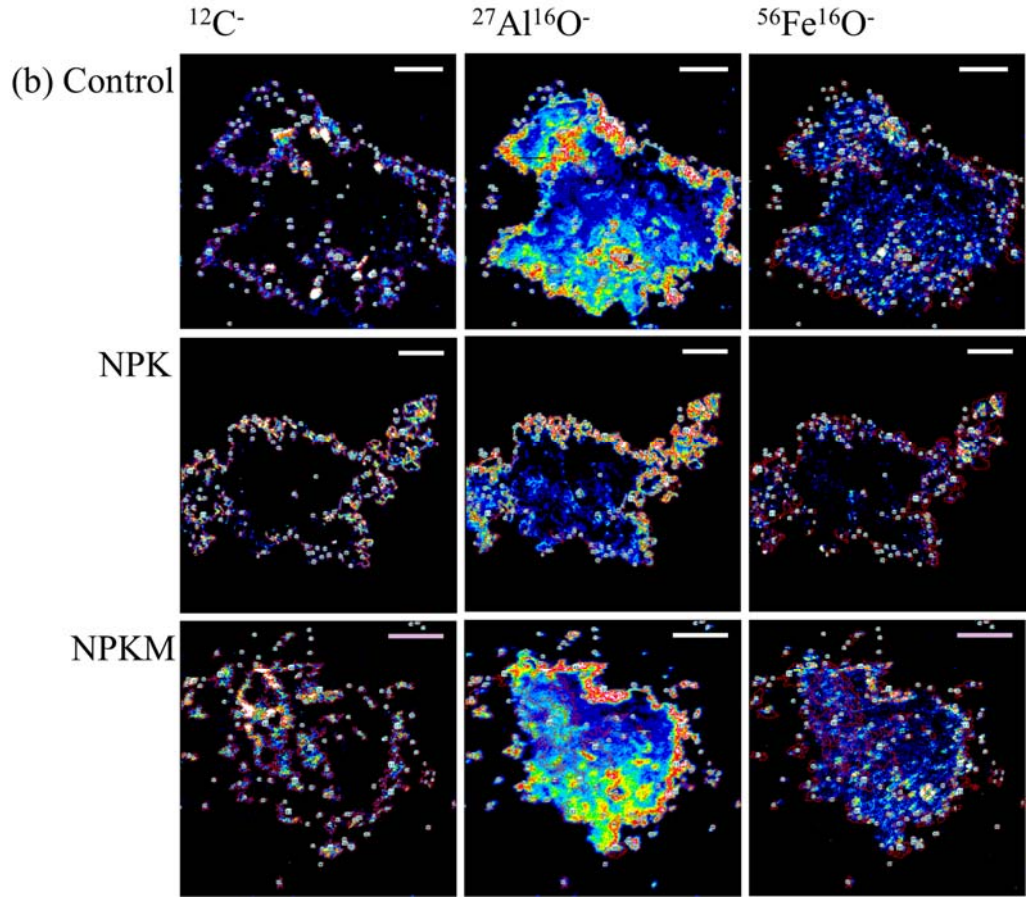
$^{12}C^-$
$^{27}Al^{16}O^-$
$^{56}Fe^{16}O^-$
(b) Control
NPK
NPKM

Fig. S2 Region of interests (ROIs) (circled by red line) of $^{12}C^-$, $^{27}Al^{16}O^-$ and $^{56}Fe^{16}O^-$ presenting on the NanoSIMS images in soil (Ferralic Cambisol) colloids extracted from three 24-year (1990-2014) long-term fertilization treatments. NanoSIMS images of (a) the $^{12}C^-$ rich ROIs of $^{12}C^-$, $^{27}Al^{16}O^-$ and $^{56}Fe^{16}O^-$ (b) the $^{12}C^-$ less rich ROIs of $^{12}C^-$, $^{27}Al^{16}O^-$ and $^{56}Fe^{16}O^-$. Control, no fertilization, 28 × 28 μm^2; NPK, chemical nitrogen, phosphorus and potassium fertilization, 30 × 30 μm^2; NPKM, chemical NPK plus swine manure fertilization, 25 × 25 μm^2. Note that the color intensity calibration bar displayed in the chemical maps corresponds to the relative concentrations of individual elements, but cannot be used to compare one element to another. Bar = 5 μm.

Table S1. Annual fertilization rates between 1990 and 2014 in Qiyang, China [a].

Treatment	Wheat				Corn			
	N (kg ha^{-1})	P (kg ha^{-1})	K (kg ha^{-1})	Swine manure (Mg ha^{-1})	N (kg ha^{-1})	P (kg ha^{-1})	K (kg ha^{-1})	Swine manure (Mg ha^{-1})
Control	0	0	0	0	0	0	0	0
NPK	27	16	31	0	63	37	73	0
NPKM	90	16	31	10-15	210	37	73	25-35

[a]Note: N fertilizer was as urea, P as calcium superphosphate, K as KCl. Swine manure was calculated in fresh weight. Control, no fertilization; NPK, chemical nitrogen, phosphorus and potassium fertilization; NPKM, chemical NPK plus swine manure fertilization.

Table S2. Quantification of $^{12}C^-$ rich ($^{12}C^-$-R) and $^{12}C^-$ less-rich ($^{12}C^-$-LR) region of interests (ROIs) [a]

		$^{12}C^-$ Rich ROIs			$^{12}C^-$ Less-Rich ROIs		
Treatment	**Replicates Number**	**ROIs Number**	**ROIs Area /Total area (%)**	**Intensity (Pixel)**	**ROIs Number**	**ROIs Area /Total area (%)**	**Intensity (Pixel)**
Control	8	312	7.47	>90	457	40.18	40-90
NPK	6	567	10.80	>90	532	27.64	40-90
NPKM	6	479	8.23	>50	596	37.99	30-50

[a]Note: Control, no fertilization; NPK, chemical nitrogen, phosphorus and potassium fertilization; NPKM, chemical NPK plus swine manure fertilization.

Table S3. Fe mineral standards used in the fitting of Fe K-edge XANES spectra

Fe mineral standards	Mineral type	Chemical formula	Origin	References
Ferrous sulfate	Inorganic ferrous oxides	$FeSO_4 \cdot 7H_2O$	Aladdin, CAS:7782-63-0	-
Ferrous oxalate	Organic ferrous oxides	$FeC_2O_4 \cdot 2H_2O$	Aladdin, CAS:6047-25-2	-
Ferric sulfate	Inorganic ferric oxides	$Fe_2(SO_4)_3 \cdot 2H_2O$	Aladdin, CAS:10028-22-5	-
Ferric oxalate	Organic ferric oxides	$Fe_2(C_2O_4)_3 \cdot 5H_2O$	Aladdin, CAS: 2944-66-3	-
Goethite	Iron Oxide	α-FeOOH	Synthetic	Schwertmann & Cornell (2007b)
Hematite	Iron Oxide	α-Fe_2O_3	Synthetic	Yen et al. (2002) Schwertmann & Cornell (2007c)
Ferrihydrite	Iron Oxide	$Fe_5HO_8 \cdot 4H_2O$	Synthetic	Michelet al. (2007) Schwertmann & Cornell (2007a)
Maghemite	Iron Oxide	γ-Fe_2O_3	Synthetic	Wang et al. (2008) Schwertmann & Cornell (2007d)

References

Michel, F.M., Ehm, L., Antao, S.M., Lee, P.L., Chupas, P.J., Liu, G., Strongin, D.R., Schoonen, M.A.A., Phillips, B.L., and Parise, J.B.: The structure of ferrihydrite, a nanocrystalline material, Science, 316, 1726-1729, 2007.

Mueller, C.W., Kölbl, A., Hoeschen, C., Hillion, F., Heister, K., Herrmann, A.M., and Kögel-Knabner, I.: Submicron scale imaging of soil organic matter dynamics using NanoSIMS-From single particles to intact aggregates, Org. Geochem., 42, 1476-1488, 2012.

Schwertmann, U., and Cornell, R.M.: Ferrihydrite, Iron Oxides in the Laboratory, Wiley-VCH Verlag GmbH, pp. 103-112, 2007a.

Schwertmann, U., and Cornell, R.M.: Goethite, Iron Oxides in the Laboratory, Wiley-VCH Verlag GmbH, pp. 67-92, 2007b.

Schwertmann, U., and Cornell, R.M.: Hematite, Iron Oxides in the Laboratory, Wiley-VCH Verlag GmbH, pp. 121-134, 2007c.

Schwertmann, U., and Cornell, R.M.: Maghemite, Iron Oxides in the Laboratory, Wiley-VCH Verlag GmbH, pp. 141-142, 2007d.

Wang, X.G., Liu, C.S., Li, X.M., Li, F.B., and Zhou, S.G.: Photodegradation of 2-mercaptobenzothiazole in the γ-Fe_2O_3/oxalate suspension under UVA light irradiation, J. Hazard. Mater., 153, 426-433, 2008.

Yen, F.S., Chen, W.C., Yang, J.M., and Hong, C.T.: Crystallite size variations of nanosized Fe_2O_3 powders during γ- to α-phase transformation, Nano Lett., 2, 245-252, 2002.